J. exp. Biol. **124**, 259–285 (1986)
Printed in Great Britain © *The Company of Biologists Limited 1986*

SLOW SYNAPTIC TRANSMISSION IN FROG SYMPATHETIC GANGLIA

BY P. R. ADAMS[1], S. W. JONES[1], P. PENNEFATHER[1], D. A. BROWN[2], C. KOCH[3] AND B. LANCASTER[1]

[1]*Department of Neurobiology and Behavior, SUNY Stony Brook, NY 11794, USA,* [2]*Department of Pharmacology, School of Pharmacy, Brunswick Square, London, UK* and [3]*Whittaker College, MIT, Cambridge, MA, USA*

SUMMARY

Bullfrog ganglia contain two classes of neurone, B and C cells, which receive different inputs and exhibit different slow synaptic potentials. B cells, to which most effort has been directed, possess slow and late slow EPSPs. The sEPSP reflects a muscarinic action of acetylcholine released from boutons on B cells, whereas the late sEPSP is caused by a peptide (similar to teleost LHRH) released from boutons on C cells. During either sEPSP there is a selective reduction in two slow potassium conductances, designated 'M' and 'AHP'. The M conductance is voltage dependent and the AHP conductance is calcium dependent. Normally they act synergistically to prevent repetitive firing of action potentials during maintained stimuli. Computer simulation of the interactions of these conductances with the other five voltage-dependent conductances present in the membrane allows a complete reconstruction of the effects of slow synaptic transmission on electrical behaviour.

INTRODUCTION

This chapter is concerned with slow synaptic transmission in amphibian sympathetic neurones. Although these forms of synaptic influence are indeed slow, slowness is not their most essential characteristic. Because the nature of the synaptic influence is more subtle than simple transmission of the nerve impulse from cell to cell the term 'neuromodulation' is often used. Although the forms of neuromodulation to be discussed are subtle, they can be quite striking under certain circumstances. Furthermore, their mechanisms are both complex and precise.

The frog lumbar sympathetic ganglia lie along two chains which are the most caudal extension of the sympathetic nervous system. Each ganglion is a collection of densely packed cells varying in colour from light yellow to deep orange. The nerve entering the ganglion (from higher up in the chain) contains axons that synapse on cells within the ganglion, as well as axons that pass through to synapse in more caudal ganglia. Most studies have been done on the largest, most caudal ganglia numbered IX and X (Kuba & Koketsu, 1978). Axons synapsing on cells in these ganglia all arise from preganglionic motoneurones in the spinal cord, but enter the chain at

Key words: sympathetic ganglion, slow EPSP, muscarinic receptor.

two different levels and exhibit different conduction velocities. Axons entering the chain rostral to the VI ganglion are moderately rapidly conducting ($2{\cdot}4\,m\,s^{-1}$) and are called B axons. Axons entering the chain at more caudal locations conduct slowly ($0{\cdot}4\,m\,s^{-1}$) and are C axons (Dodd & Horn, 1983*a*). These arrangements are sketched in Fig. 1.

These two classes of axon synapse selectively on two classes of cells found higgledy-piggledy within the ganglion. B axons synapse on cells of diameter 30–60 μm, which are called B cells, whereas C axons synapse on 15–40 μm C cells. B cells typically receive only one suprathreshold axon input, whereas C cells may be multiply innervated. In both cases, the incoming axons spiral round the axon hillock, establishing synapses there and over the cell body (Weitsen & Weight, 1977). There are no dendrites, so all synapses are located close to recording electrodes on or in the cell body. There are typically 40 boutons per cell, though this probably varies with cell size, such that synaptic density is rather constant (Sargent, 1983).

B CELLS

The most important difference between B and C cells is the nature of the synaptic action exerted by stimulation of their incoming axons. Stimulation of the axon to a

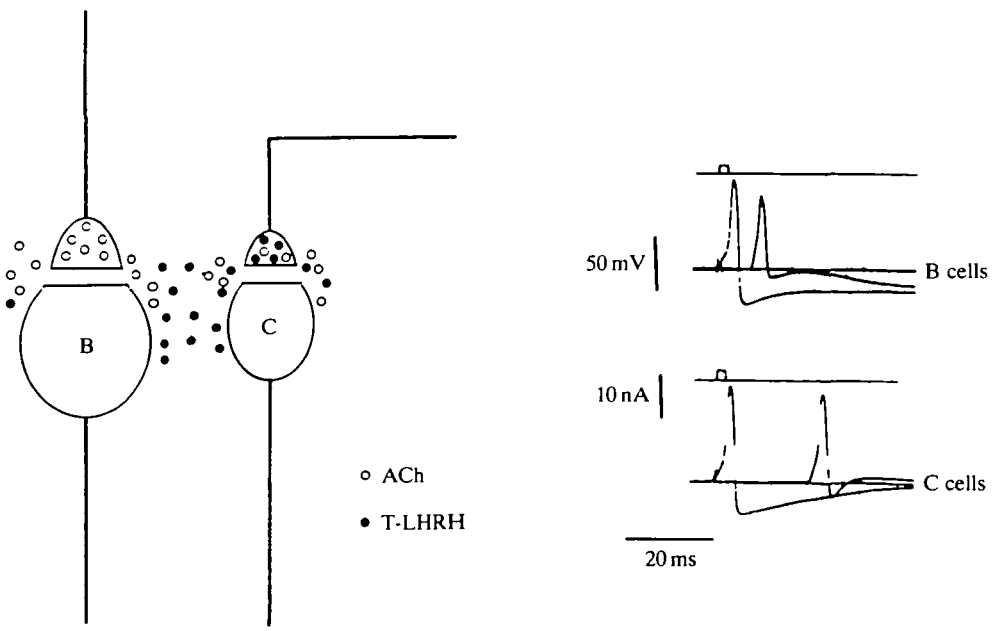

Fig. 1. Diagram of synapses on B and C cells. Synapses on B cells release only acetylcholine (ACh). Synapses on C cells release both ACh and T-LHRH. T-LHRH, unlike ACh, can diffuse within the ganglion. The righthand part of the diagram shows direct and orthodromic spikes in B and C cells. The direct spikes, triggered by brief current pulses monitored in the upper traces in each pair, precede and are larger than the orthodromic spikes. Note the two-component decay of the B cell direct spike afterhyperpolarization compared to the smooth decay of the C cell afterhyperpolarization. Also note the much slower orthodromic conduction velocity in C cells.

B cell results in two successive depolarizations, the fast and slow EPSPs. The fast EPSP reaches a peak in 1–2 ms and decays with a time constant roughly equal to the cell membrane time constant, about 15 ms. It is generated by a brief inward current, the fast EPSC, which lasts about 20 ms. The slow EPSP starts rising at about 50–100 ms after the end of the fEPSP, reaches a peak after 1–2 s, and lasts about 1 min. The underlying inward current, the slow EPSC, has a similar time course. The fast and slow EPSPs are both cholinergic but differ in every other respect. The fast EPSP is generated in the same way as the endplate potential at the nerve–muscle junction. It reflects the sum of numerous, almost synchronous fmEPSCs peppered all over the cell. Because mEPSCs have very similar time courses to the fEPSC itself it is likely that each constituent mEPSC is independently generated, probably 1–2 per bouton. The exponential decay of the fEPSC reflects the random distribution of the individual channel openings. The channels have very similar conductances in B and C cells (approx. 30 pS) but the mean open time is about twice as long in C cells as in B cells (Marshall, 1985). Unlike the situation in the endplate, the channel open time shows very little voltage sensitivity (Kuba & Nishi, 1979; MacDermott, Connor, Dionne & Parsons, 1980). One curious feature of these ganglion cells is that the mEPSCs are very scattered in amplitude despite the apparently equivalent location of all the boutons. This could reflect variability in vesicle size or filling, effective receptor density (but see Land, Salpeter & Salpeter, 1981) or details of geometry. The postsynaptic receptors are nicotinic, and are blocked by curare in an apparently exclusively competitive manner (D. Lipscombe & H. P. Rang, personal communication). These receptors seem to be located almost exclusively under the boutons (Marshall, 1981).

The receptors mediating the slow EPSP are muscarinic, for the response is completely blocked by atropine in the 10–100 nmol l^{-1} range. It is not yet known whether the receptors are principally of the M1 or M2 type (i.e. very sensitive or not to pirenzipine), nor is their anatomical distribution known. In cardiac muscle, Hartzell (1980) has shown by autoradiography that muscarinic ligand is found all over the cell surface but he was unable to decide if the receptors were located exclusively under terminals or at random on the surface, and similar ambiguities might attend on autoradiographic experiments in ganglion cells.

Nevertheless, the differences in behaviour of the amplitudes of the fast and slow EPSCs during repetitive stimulation may offer some clue as to localization. The first EPSC in a train is normally the largest, and even if the stimulation frequency is high enough to produce overlap, little summation occurs. In contrast, the slow EPSC evoked by a single stimulus is very small, and grows *pari passu* with the number of shocks in a train, until it reaches a limit governed by the available M-current (see below). The simplest interpretation of this is that the slow EPSP is generated by 'excess' acetylcholine (ACh), that comes off nicotinic receptors and escapes the gauntlet of acetylcholinesterase (AChE). Saturation of receptors and esterase (and hence availability of excess ACh) is more likely to occur with repetitive stimulation. This interpretation is supported by the observation that administration of anti-cholinesterases increases the amplitude of the slow EPSC much more than that of

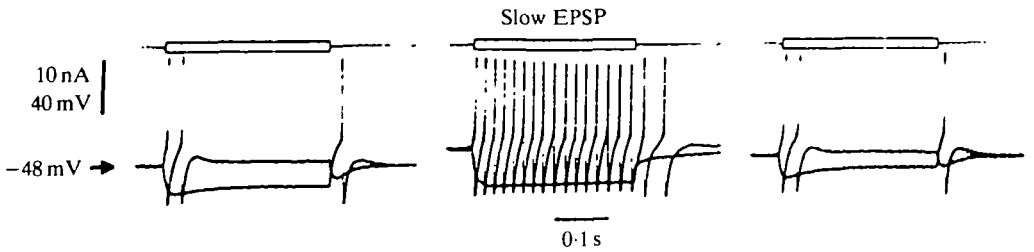

Fig. 2. Excitability changes during the slow EPSP. The lefthand trace shows the control response to a long current pulse, the middle trace the response to the same current at the peak of the slow EPSP (note the small depolarization) and the righthand trace the response 2 min after the beginning of the slow EPSP.

the fast EPSP. It may be suggested, then, that the nicotinic receptors get 'first pick' of the released ACh, and that muscarinic receptors, possibly because of an extra-boutonal location or because of a slow forward binding rate, get the crumbs from the table.

The fEPSC is normally large enough to depolarize the cell to the threshold, firing an action potential whose time course (itself greatly influenced by the underlying EPSC) largely obscures the subsequent sEPSP. In a tiny proportion of cells, this action potential can itself trigger a 'recurrent' EPSP. This most rare recurrent EPSP is probably cholinergic, because it is blocked by curare, and so it is probably due to an autapse.

If the fEPSP is suppressed (e.g. with curare) the sEPSP is found to be far too small to reach threshold, even when evoked by optimally effective tetani (e.g. 10–20 stimuli at 20 Hz). The slow EPSP is therefore useless in procuring straightforward transmission through the ganglion. It appears that the membrane depolarization occurring during the slow EPSP is not itself the important feature of this synaptic action, but instead it is a striking change in the 'electrical personality' of the nerve cell. This is shown in the experiment in Fig. 2. The first part shows the typical response of a B ganglion cell to a weak maintained depolarizing current pulse. The cell fires a couple of spikes and then falls silent. The same stimulus is then applied at the peak of the slow EPSP, and now the cell gives a vigorous repetitive discharge. One minute later the cell's behaviour has returned to normal. Merely depolarizing the cell (for example by passing current) to the level attained during the sEPSP produces little or no change in the firing pattern of the cell. Furthermore, the effect is not simply due to an increase in membrane resistance, since it cannot be mimicked by just increasing the depolarizing stimulus current strength (although there is an increase in input resistance during the slow EPSP or during muscarinic stimulation which can by itself make the cell more excitable; Schulman & Weight, 1976). Because the spiking behaviour of nerve cells reflects the participation of a range of voltage-dependent conductances, it seems intuitively likely that the major effect of the sEPSP must be to modulate one or more of the voltage-dependent conductances of these cells (Koketsu, 1984). Later in this chapter the details of this modulation will be described, and furthermore it will be shown that this modulation is indeed

adequate to explain the observed modification of repetitive firing behaviour during slow synaptic transmission.

C CELLS

Stimulation of the axon(s) innervating a C cell results in three successive potential waves: a fast EPSP closely resembling that seen in B cells, a fast IPSP reaching a peak in 100 ms and lasting 1 s or so, and a late slow EPSP peaking in 30 s and lasting for 5 min. The fast IPSP is muscarinically mediated and reflects a transient increase in permeability to potassium ions (Dodd & Horn, 1983*b*). Because it tends to hyperpolarize the cell towards E_K (approx. -100 mV) it is inhibitory in effect. Little is known about the channels involved, though they may resemble those responsible for a very similar muscarinic IPSP in heart muscle (Sakmann, Noma & Trautwein, 1983). In heart muscle the muscarinic K^+ channels are stimulated by ACh only within the recording patch electrode in the on-cell configuration, arguing against the participation of a second messenger. However, recent work has nevertheless implicated a GTP-binding protein in the receptor–channel linkage (Pfaffinger *et al.* 1985; Breitwieser & Szabo, 1985).

Kuffler and his colleagues (Jan & Jan, 1982; Jan, Jan & Kuffler, 1979, 1980; Kuffler & Sejnowski, 1983) have provided convincing evidence that the late slow EPSP is mediated by release of a peptide resembling mammalian LHRH. The evidence is as follows: (1) boutons on C cells, but not those on B cells, stain for M-LHRH; (2) an M-LHRH-like peptide is released by preganglionic nerve stimulation in a calcium-dependent manner; (3) the late sEPSP can be mimicked by application of M-LHRH to the cells; (4) M-LHRH antagonists block both the effects of applied M-LHRH and the late slow EPSP itself. Subsequently Eiden & Eskay (1980) and Sherwood *et al.* (1983) showed that the M-LHRH-like peptide in the ganglion is not M-LHRH, but closely resembles the LHRH of salmon brain, T-LHRH. Frog brain contains both M-LHRH- and T-LHRH-like peptides. Subsequently it was shown that T-LHRH closely, and very potently, mimics the late sEPSP, and that T-LHRH-based antagonists block it (Jones, Adams, Brownstein & Rivier, 1984; Jan & Jan, 1982). At present, therefore, T-LHRH or a very similar peptide is the most likely candidate for the transmitter of the late sEPSP.

Because boutons on C cells stain both for LHRH and for choline acetyltransferase, and stimulation of the same set of axons releases both LHRH-like and ACh-like material, it is suspected that both transmitters are co-released from the same boutons (which contain both small clear vesicles and large dense-core granules). Additional evidence for this comes from experiments in which fEPSPs and late sEPSPs could be fractionated by varying the stimulus strength (Jan & Jan, 1982). It was found that the different components of the fEPSPs and the late sEPSPs had identical stimulus thresholds, showing that the same axon generated both responses. It remains possible, however, that the two transmitters are not released precisely in parallel in both spatial and temporal coincidence. Certain boutons may release more or less of one transmitter, and peptide release may be slower than ACh release. Indeed, part of

the slow rise time of the late sEPSP could reflect slow diffusion or might reflect sluggish coupling of peptide release to calcium entry, such as would occur if hydrolytic processing were necessary prior to release.

Dodd & Horn (1983*a*,*b*) have shown that the excitability of C cells changes dramatically during the late sEPSP in a very similar manner to that discussed above for muscarinic modulation of B cells. Jones (1984) has shown that the biophysical mechanisms for LHRH action on C cells are identical, in at least one important regard, to those for the sEPSP in B cells.

C–B interactions

If axons innervating C cells are stimulated repetitively, a late sEPSP can also be recorded in B cells. Although this late EPSP is somewhat slower in B cells than in C cells, it is actually more reliably seen, corresponding to the greater variability of C cell responses to LHRH-like substances. L. Y. Jan & Y. N. Jan have shown that the late sEPSP in B cells reflects extracellular diffusion of peptide from boutons synapsing on C cells. This is an important demonstration that the anatomical and physiological 'polarity' of synapses need not coincide.

During the C-evoked late sEPSP in B cells there is a dramatic enhancement of directly evoked repetitive firing just as is seen with the sEPSP, and the biophysical mechanisms for these effects are identical (Adams & Brown, 1980; Jones *et al.* 1984). The C-evoked B cell late sEPSP therefore represents a clear-cut example of heterosynaptic modulation of orthodromic transmission. Unlike the heterosynaptic facilitation seen in *Aplysia* sensory neurones it is postsynaptic in origin.

THE VOLTAGE-DEPENDENT CONDUCTANCES OF B CELLS

To understand the modification of discharge pattern during the sEPSP it is essential to characterize all the major voltage-dependent conductances present in the somatic-axon-hillock membrane, partly because any of these might be targets for muscarinic action, and partly because during normal cell firing all of them may be brought into play and must therefore be quantitatively modelled in a final synthesis. This task has occupied the bulk of our energies over the last few years and is now nearing completion. The observed conductances fall into three groups: those for sodium, calcium and potassium.

The sodium conductances have been characterized by a whole-cell switch-clamp method in dissociated ganglion cells lacking visible processes. At first glance the sodium currents observed after suppression of K^+ and Ca^{2+} currents look very like those seen in squid axon or vertebrate node of Ranvier. The most obvious difference is that the currents are somewhat slower at all potentials, and require rather larger (by 30 mV or so) depolarizations to produce equivalent degrees of activation or inactivation.

A closer scrutiny has revealed that there are probably two separate Na^+ conductance systems. The major one (70–80 % of the total current) is quite classical, showing rapid inactivation and block by tetrodotoxin (TTX) in the nanomolar

range. The minor component inactivates somewhat more slowly and is much less sensitive to TTX. Perhaps the most striking difference is that the minor, but not the major, component is sensitive to submillimolar amounts of cadmium (S. W. Jones, unpublished results). Similar distinctions are seen in vertebrate sensory cells (Bossu & Feltz, 1984).

So far only one calcium conductance has been described. It activates rapidly (within milliseconds) in the potential range −25 to +50 mV, and shows extremely slow current-dependent inactivation. Of the three types of calcium current described by Nowycky, Fox & Tsien (1983), it most closely resembles the L-form. Large prolonged hyperpolarizations do not reveal additional forms of calcium current and, with one possible exception, calcium entry *via* this pathway seems adequate to account for the observed calcium-dependent K^+ currents. The calcium current is not very well blocked by simple calcium omission, because of residual calcium and shifts in activation voltage. However, it is well blocked by cadmium, manganese, cobalt or nickel. Because any one alone of these procedures may have independent side effects, a demonstration of calcium dependence is best achieved with a battery of tests.

Five different types of K^+-conductance have been described (Adams, Brown & Constanti, 1982*a*; Adams, Constanti, Brown & Clark, 1982*c*; Pennefather, Jones & Adams, 1985*a*; Pennefather, Lancaster, Adams & Nicoll, 1985*b*; Lancaster & Pennefather, 1986). One of these, which we call I_K, is similar to the classical delayed rectifier current of squid axon, node of Ranvier and molluscan cell bodies. Its hallmarks are sigmoidal activation, very slow but complete voltage-dependent inactivation and sensitivity to millimolar external tetraethylammonium (TEA). It is rather slower than the nodal delayed rectifier (which, however, does exhibit both fast and slow components; Dubois, 1981). I_K is not reduced by omitting external calcium; indeed this procedure enhances it, possibly through a surface potential modification.

Two of the other K currents of B cells are also fairly classical. There is a rapid, transient, low-threshold K current strongly resembling the A current of invertebrate neurones (Connor & Stevens, 1971; Neher, 1971), and a rapid, voltage-dependent, calcium-activated current essentially identical to that of chromaffin or muscle cells (Marty, 1981; Adams *et al.* 1982*c*; Barrett, Magleby & Pallotta, 1982). We call the latter current I_C so as to avoid confusion with the other calcium-activated K^+ current I_{AHP} (see below). The term $I_K(Ca)$ will be used to refer to any type of Ca^{2+}-activated K^+ current when the exact type is immaterial, or unknown.

Like I_K, but unlike the other K^+ currents, I_C is blocked by millimolar TEA. It can be separated from I_K by various tests. It activates much more rapidly, it is mostly blocked by calcium removal, metallic calcium antagonists or charybdotoxin (see Miller, Moczydlowski, Latorre & Phillips, 1985). Following depolarizations that activate both I_C and I_K, the major rapid outward tail current that follows repolarization to rest potential is a mixture of I_C and I_K, which, because of their somewhat similar kinetics and voltage dependence, can be quite difficult to separate. However, tail current following either very brief (1 ms) or very long (1 min) depolarizations consists almost exclusively of I_C, because I_K either has not had time

to activate or has completely inactivated. It is, in fact, rather surprising that the tail currents in these two situations should be rather similar, because the intracellular calcium concentration and distribution must be very different. Nevertheless the kinetics of I_C are roughly compatible with a simplified version of the scheme proposed by Moczydlowski & Latorre (1983) from data obtained with reconstituted single channels:

$$Ca + R \rightleftharpoons CaR \rightleftharpoons CaR^* \rightleftharpoons Ca_2R^*,$$

where R^* is the open form of the channel and the calcium binding reactions are assumed to be very fast. This represents a reduced form of a more elaborate scheme developed by Magleby & Pallotta. In this scheme the voltage dependence of channel opening reflects voltage dependence of Ca^{2+} binding. For example, in bullfrog cells the steady-state conductance evoked by small increases in intracellular calcium grows e-fold for 11 mV membrane depolarization (Adams *et al.* 1982*c*).

Although inactivation of I_C has been reported, it is very slow (Pallotta, 1985), as is that of the calcium current itself. It is thus quite surprising that there are two reports that an I_C-like current can show extremely rapid inactivation under certain circumstances (MacDermott & Weight, 1982; Brown, Constanti & Adams, 1982). In both sets of experiments, depolarization to between −20 and 0 mV from a rather negative holding potential elicited a large transient outward current that was blocked by Ca^{2+} omission, metallic Ca^{2+} antagonists or TEA. It is possible that this represents a distorted form of I_C caused by series resistance problems, poor space clamp or potassium accumulation, although Ca^{2+}-dependent transient outward currents have been described in other systems (Salkoff, 1983).

The remaining two potassium currents of B cells are less familiar, though they probably both have counterparts in many other types of nerve cell. They are both small, slow currents that can be overlooked in conventional voltage-clamp experiments. One, I_M, is purely voltage dependent, and the other, I_{AHP}, is purely Ca^{2+} dependent. In fact, strictly speaking, I_{AHP} is not a voltage-dependent current at all, since its 'voltage dependence' derives exclusively from that of calcium entry, but operationally it belongs to this family of currents.

I_M begins to activate at a rather negative potential, about −60 mV, and is almost fully activated at the threshold for the sodium current. The activation–deactivation time constant is about 150 ms at −35 mV, but becomes much faster at more negative potentials. The reversal potential for I_M is about −85 mV, which is slightly more positive than the value estimated for I_{AHP}, possibly due to K^+ accumulation in the narrow glia–neurone ('Frankenhauser–Hodgkin') space. I_M does not inactivate even during depolarizations lasting tens of minutes.

I_{AHP} has only been studied as a tail current following very brief depolarizations (such as action potentials or voltage-clamp steps) because it requires large depolarizations which elicit currents (particularly I_C) which dwarf I_{AHP}. However, it is clear from envelope measurements that I_{AHP} can be maximally activated by pulses of 1–2 ms duration. The late tail current following such brief depolarizations or single

spikes decays approximately exponentially with a time constant of 250 ms. Following a burst of spikes, I_{AHP} decays more slowly though its initial amplitude is much the same.

I_{AHP} is abolished by blocking Ca^{2+} entry (Fig. 3), suggesting that it is calcium dependent. If I_{AHP} is *defined* as the slow current that is blocked by calcium antagonists, it may show a rising phase (Tokimasa, 1984). However, clear definition of the early part of the tail as a difference current is difficult because of the effects of Ca^{2+} depletion on other very large early tail currents.

I_{AHP} is partially blocked by the bee venom toxin apamin (see also Hugues *et al.* 1982; Romey & Lazdunski, 1984), which blocks Ca^{2+}-activated K^+ permeability in hepatocytes (Jenkinson, Haylett & Cook, 1983). Cook & Haylett (1985) have recently shown that a variety of bisquaternary compounds such as pancuronium, curare and hexamethonium not only block $G_K(Ca)$ in liver cells but also compete at the apamin binding site. These compounds also block I_{AHP} in bullfrog neurones (Nohmi & Kuba, 1984; Pennefather *et al.* 1985*a*).

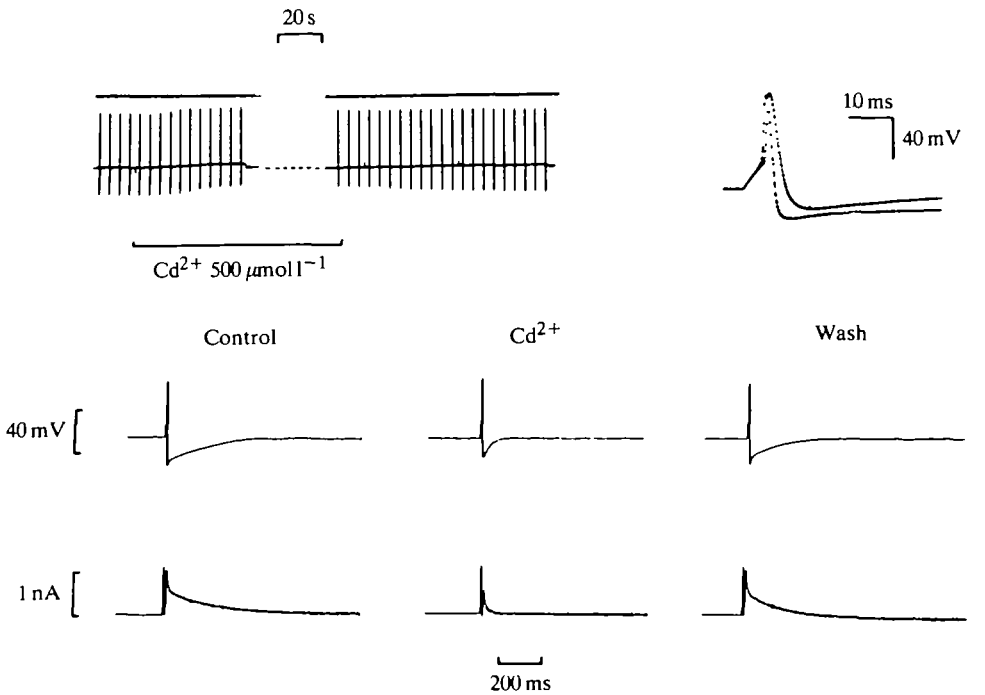

Fig. 3. Effects of calcium influx blockade on spikes in a B ganglion cell. The upper row shows action potentials elicited by a brief current pulse. The chart recording on the left shows the block by cadmium of the spike afterhyperpolarizations (downward excursions) and the oscilloscope record on the right shows superimposed spikes in the absence and presence of cadmium. The middle traces show the effects of cadmium on the slower components of the spikes. In the bottom row the hybrid clamp protocol was used, so that the records are of the currents following a clamp to the resting potential imposed at the peak of the early afterhyperpolarization. This current is mostly I_{AHP}.

TRANSMITTER SENSITIVITY OF I_M AND I_{AHP}

The B cells thus exhibit at least seven separate voltage-dependent conductances. Each is presumably mediated by distinct ionic channels (though so far only those for I_C and I_K have been clearly identified in single-channel recordings). However, of these seven only the two slow, small K^+ currents, I_M and I_{AHP}, are clearly influenced by the activation of muscarinic receptors. An example of these effects is shown in Fig. 4. In Fig. 4A the cell was held at −60 mV and stepped at 20 mV positive or negative. The positive step elicited a time-dependent outward current relaxation, I_M. This relaxation was reversibly almost abolished by addition of muscarine. The positive step does not elicit I_{AHP} because it is not large enough to open calcium channels. Occasionally in this type of experiment the positive step does trigger an abortive poorly clamped action potential, in which case I_M can be contaminated by I_{AHP} and appear spuriously Ca^{2+} dependent.

Fig. 4B shows what happens when a full spike is deliberately triggered. The bottom traces reveal that the spike is followed by a prolonged afterhyperpolarization (AHP), which is reduced and shortened in muscarine. This effect is partly due to an increase in membrane leak conductance, visible in Fig. 4A and discussed below. However, it is also partly due to a decrease in I_{AHP} itself, as shown by the 'hybrid clamp' experiment in the top row of Fig. 4B. This shows the outward current tail that flows if the membrane potential is returned to rest at the peak of the AHP. The I_{AHP} tail is reduced to about 70 % of control amplitude by addition of muscarine, with little change in time course. Since muscarine has no effect on ganglion cells in which Ca^{2+} current has been isolated by blocking or removing most Na^+ and K^+ current (P. R. Adams, unpublished observations; see also Tokimasa, 1985), the reduction in I_{AHP} is probably not secondary to attenuation of Ca entry. This is not certain because the I_C experiments involve the use of TEA which may block muscarinic receptors.

The magnitudes of the effects of muscarine on I_M and I_{AHP} seen in Fig. 4 are quite typical. Even high doses of muscarine (100 μmol l^{-1}) do not block more than 80–90 % of I_M or more than 10–30 % of I_{AHP}, even though the half blocking concentration for muscarine acting on I_M is about 1 μmol l^{-1}. It is not known why this should be so, or whether the muscarine-resistant fraction of I_{AHP} corresponds to the apamin-sensitive fraction.

Muscarinically mediated reductions of I_M or I_{AHP} can also occur physiologically (i.e. following presynaptic ACh release). After a single nerve shock, only a small fraction of the total M conductance is turned off, but optimal trains can block nearly all of it. If the cell is held at a potential where there is standing M current (i.e. −60 mV or more positive) the partial shut-down of M conductance leads to a transient inward current which accounts for virtually all the sEPSC (Adams & Brown, 1982). This endows the sEPSC with its paradoxical voltage dependence, first noted by Weight & Votava (1970), such that it is enhanced by depolarizing the membrane. Furthermore, because E_K is normally negative to the activation range for G_M, it is virtually impossible to reverse the sEPSC.

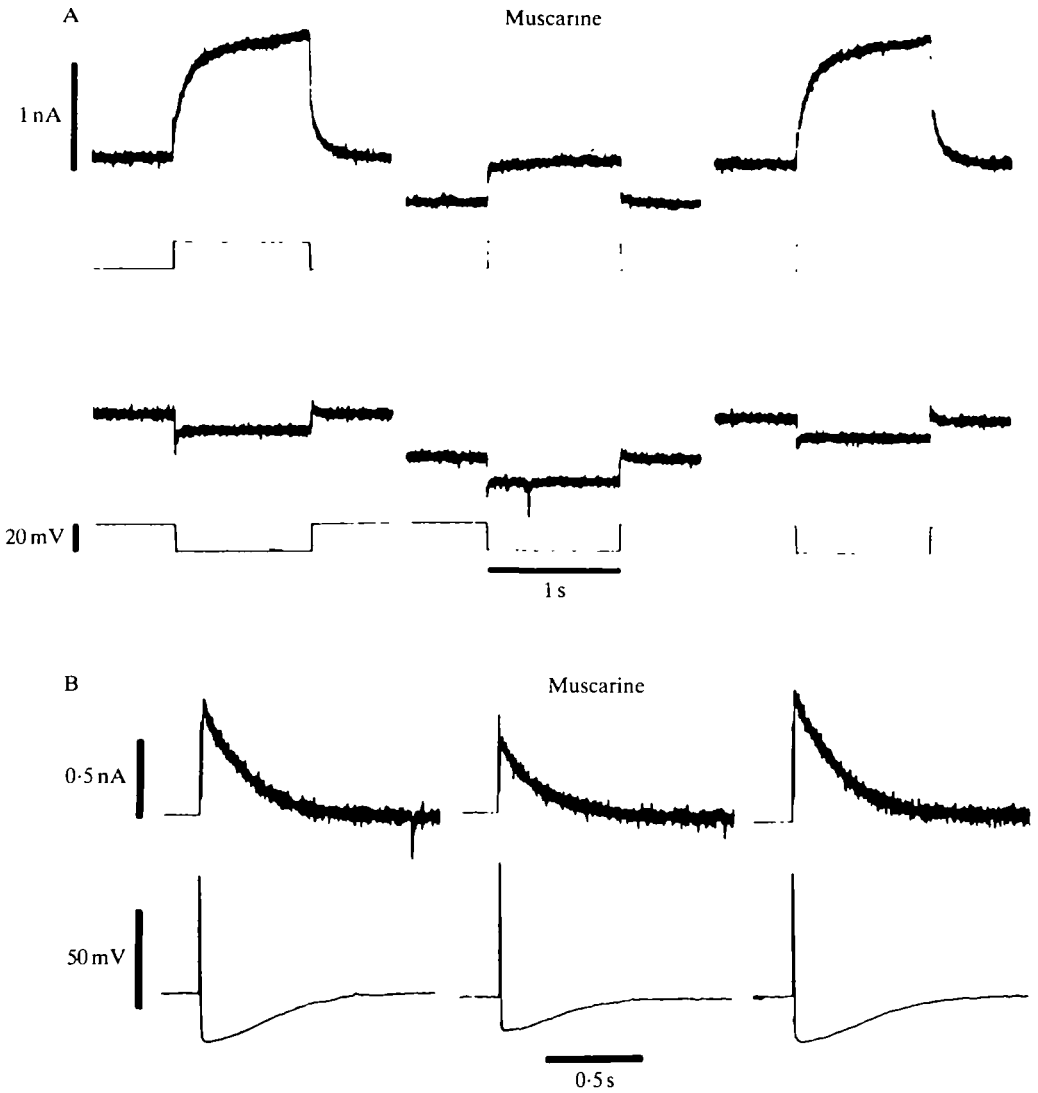

Fig. 4. Effects of muscarine ($100\,\mu mol\,l^{-1}$), applied from a pressure pipette, on I_M, I_{AHP} and I_{LEAK} in a B cell. (A) The effect on I_M (upper traces) and I_{LEAK} (lower traces); (B) the effects on I_{AHP} (top) and the spike afterhyperpolarization (lower). The left-hand traces show controls, the righthand traces show recoveries. See text for further explanation.

The effects of muscarine and related agonists on I_M and I_{AHP} are clearly mediated by muscarinic receptors for they are blocked by low concentrations of atropine. However, a variety of other receptors are also coupled in a similar manner to I_M and I_{AHP}. These are LHRH receptors, substance P receptors and nucleotide receptors. The effect of T-LHRH is illustrated in Fig. 5, which is patterned after Fig. 4. T-LHRH, like muscarine, produces a large reduction in I_M and a small reduction in I_{AHP}. T-LHRH is thought to be the natural transmitter for the late sEPSP, and

indeed a very similar reduction in I_M occurs during this synaptic response. The effects of T-LHRH and related compounds, as well as those of the synaptically released transmitter, are blocked by antagonists based on the M-LHRH or T-LHRH

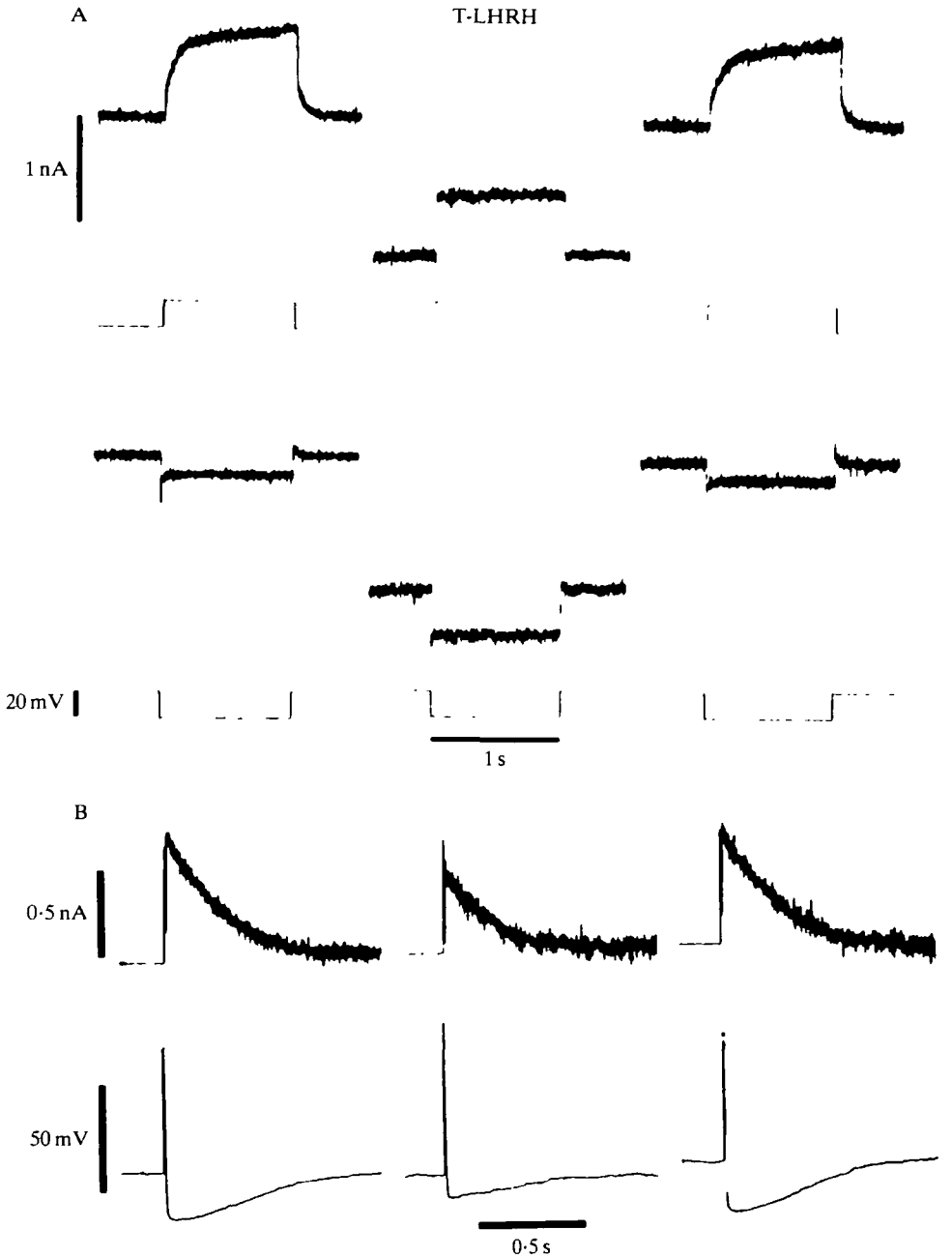

Fig. 5. Effects of pressure-applied T-LHRH (100 μmol l^{-1} in pipette) on I_M, leakage conductance and I_{AHP}. See text for further description.

structures, which do not affect the responses to muscarine. Therefore, a quite distinct LHRH receptor must exist in the cell membrane and be coupled to I_M and I_{AHP}.

The description of the other receptor types is less complete, largely because of the lack of specific antagonists. Substance P effects on I_M are rather variable from cell to cell, some cells responding to concentrations as low as $1\,nmol\,l^{-1}$ (being the most potent of any drug effects on this system), while other cells do not respond even at $10\,\mu mol\,l^{-1}$ (Adams, Brown & Jones, 1983; Jones *et al.* 1984). This variability may reflect inconsistent desensitization or tissue penetration. Substance P attenuates the slow spike AHP (Akasu, Nishimura & Koketsu, 1983*b*) and thus probably reduces I_{AHP}.

I_M is also reduced, to about 10% of normal, by high concentrations of UTP or ATP (Adams, Brown & Constanti, 1982*b*; Akasu, Hirai & Koketsu, 1983*a*; P. Pennefather, unpublished results), whereas UDP and ADP are almost ineffective. It is not known whether one or two nucleotide receptors are involved. ATP also produces a 30% reduction in I_{AHP} (P. Pennefather, unpublished results).

These data suggest two alternative extreme pictures of the coupling of the various receptor types to the voltage-dependent conductances (Fig. 6). In the first view, each receptor is separately coupled to each channel; either as a result of a permanent physical association of all five units (four receptors and one channel) or because each channel can transiently link with activated forms of any of the receptors. In the second view, there is *never* a physical association. Instead activation of any one of the four receptor types causes changes in the concentration of one or more second messengers ('X'), which in turn affects the number of channels available for activation. Attempts to identify X have so far proved inconclusive. Intracellular injections of cyclic nucleotides or calcium failed to affect the amplitude of I_M. In the former case this could reflect rapid breakdown of the injected substances, although extracellular applications of stable or lipid-soluble analogues or of forskolin were equally ineffective. In the latter case there was evidence that Ca^{2+} did indeed reach the membrane, because activation of I_C was seen, but even here Ca^{2+} may not have reached all the membrane at adequate concentrations to inhibit I_M. Tokimasa (1985) has recently suggested that massive calcium loading *via* Ca^{2+} spikes may inhibit I_M. If Ca^{2+} is indeed involved in control of I_M, it is unlikely that calcium influx across the plasmalemma is itself the normal signal for I_M inhibition by muscarine because the effect of muscarine persists in Ca^{2+}-free solution or after addition of metallic calcium blockers. However, in several other cell types, including neurones, there is evidence that muscarinic or peptide receptor activation leads to enhanced phosphatidylinositol 4,5-bisphosphate (PIP_2) breakdown, yielding inositol trisphosphate (IP_3) and diacylglycerol (DAG) (Horwitz, Tsymbabov & Perlman, 1984). Conceivably IP_3 release also occurs in ganglion cells, resulting in Ca^{2+} efflux from endoplasmic reticulum (Streb, Irvine, Berridge & Schulz, 1983). Calcium release from such internal stores induced by caffeine or membrane depolarization is known to occur in these cells (Kuba, 1980; Adams *et al.* 1984). It will be interesting to examine the effects of IP_3 injections on ganglion cells.

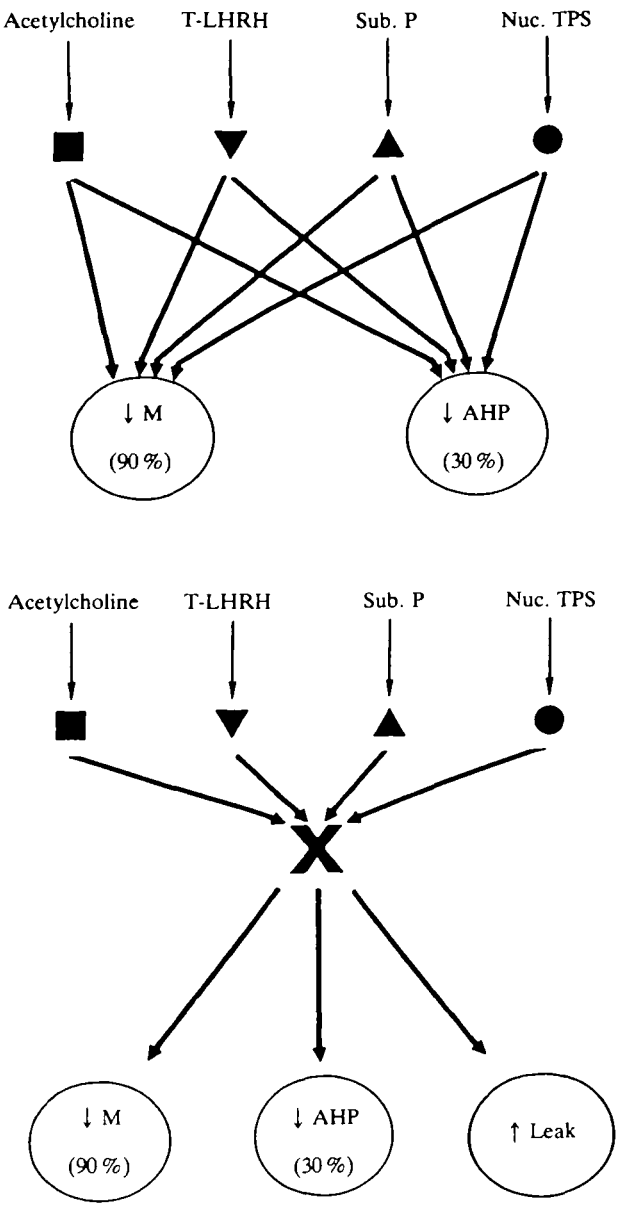

Fig. 6. Two extreme views of receptor–channel coupling in bullfrog neurones. Sub.P, substance P receptors; Nuc.TPS, nucleotide receptors; AHP, afterhyperpolarization; M, M current.

Extracellular application of DAGs to ganglion cells has so far not revealed consistent effects. However, it has been recently shown that active phorbol esters such as phorbol dibutyrate, at micromolar concentrations, affect the M system in two ways (Adams & Brown, 1986). First, they reduce the size of the available M current and, second, they block the effects of muscarine or LHRH on I_M. These effects are specific in that neither I_{AHP} nor the action potential itself are affected.

In addition, phorbol esters do not block the 'leak' increase produced by muscarine (see below). It has been shown in a variety of other systems that phorbol esters also block biochemical responses to activation of various receptors which are linked to PIP_2 breakdown. For example, in chromaffin cells phorbol esters block the muscarinically evoked intracellular release of Ca^{2+} and DAG (Vicentini *et al.* 1985). Fig. 7 sketches a way in which these various fragmentary observations might be interpreted. It suggests that receptor stimulation leads to phosphatidylinositol (PI) turnover *via* a coupling protein. C-kinase activation by phorbol ester might phosphorylate this coupling protein so as to impair the PI turnover response to receptor activation. Normally, however, release of Ca^{2+} *via* IP_3 liberation and the release of synergistically acting DAG activates C-kinase which phosphorylates some component of the M channel system. The variable or unconvincing effects of phorbol ester or calcium acting separately on M conductance would be explained by a normal requirement for simultaneous $[Ca^{2+}]_i$ and [DAG] elevation. This scheme is currently being tested in our laboratory.

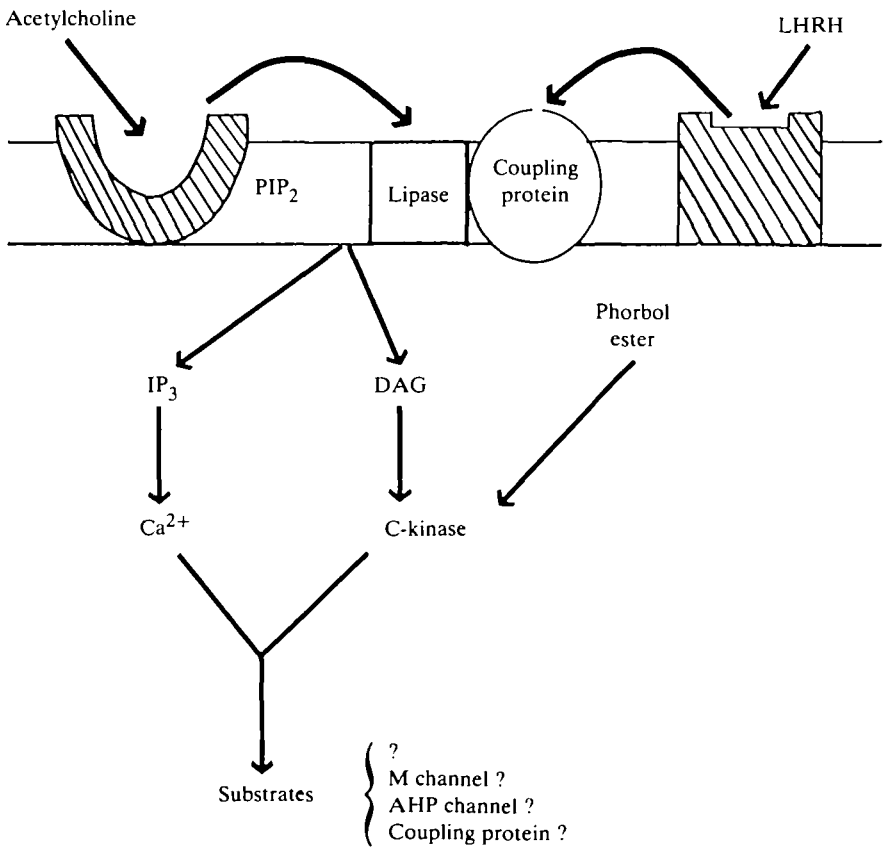

Fig. 7. Possible activation on targets of C-kinase in ganglion cells. PIP_2, phosphatidylinositol 4,5-bisphosphate; IP_3, inositol trisphosphate; DAG, diacylglycerol.

TRANSMITTER EFFECTS ON LEAKAGE

If a cell is voltage clamped at −60 mV, virtually no time-dependent, voltage-sensitive current is present, and the behaviour is almost ohmic for moderate hyperpolarizations, until a slow creep current appears below −100 mV. The slope of the I/V relationship in this range thus reflects the membrane 'leak' resistance. This leakage is rather variable, and tends to be lowest when using high-resistance, sharp microelectrodes or after 'sealing in' of the electrode. Part of the leak conductance is thus probably due to the 'hole' caused by microelectrode impalement, either the physical discontinuity itself, or general membrane effects arising from influx of extracellular medium. However, part of the leakage conductance must reflect an intrinsic membrane property, because even the very best impalements never yield input resistances above 200 MΩ. Whole-cell recording also usually yields input resistances in the negative potential region of several hundred megohms, even when the initial seal is many gigohms, is very stable, and membrane rupture appears to be clean and smooth. The intrinsic part of the leakage conductance is often increased by application of muscarinic or peptidergic agonists (e.g. Figs 4, 5). This effect is characteristically seen during prolonged application of high doses. Furthermore, it lags behind the onset and recovery of the effects of the same drug application on I_M (Jones, 1985). This suggests that the mechanism of this effect may be quite different from that on I_M or I_{AHP}, which is supported by the differential effects of phorbol esters on I_M inhibition and leakage increase. The leakage conductance increase probably involves Na^+ and/or Cl^- ions since the reversal potential is quite positive. It is thus capable of generating an inward current at potentials where I_M is inoperative. However, it is not normally seen during slow synaptic transmission, unless drastic stimulation is used (Akasu, Gallagher, Koketsu & Shinnick-Gallagher, 1984).

C CELLS

Exploration of the voltage-dependent conductances of C cells has lagged behind that of B cells, largely because of their smaller size. The action potentials of these cells lacks the characteristic break in the afterhyperpolarization (see Fig. 1) which reflects the two-component ($I_C + I_{AHP}$) tail current in B cells. Correspondingly, hybrid clamp experiments reveal a tail current which decays much faster than I_A, but which is TEA and probably calcium insensitive (S. W. Jones, unpublished observation).

C cells possess a normal M current, with almost identical kinetics and voltage sensitivity to that of B cells. However, I_M in these cells is *not* reduced by muscarine. Thus although I_M was first defined by sensitivity to muscarinic receptor activation, this is not a necessary characteristic. A muscarine-insensitive I_M is also found in cultured sensory ganglion cells (Barry, Werz & Macdonald, 1983).

I_M in C cells is sensitive to LHRH agonists, though less consistently so than in B cells. Application of LHRHs to cells held at −60 mV or more negative sometimes unexpectedly produces an *outward* current accompanied by a *decrease* in

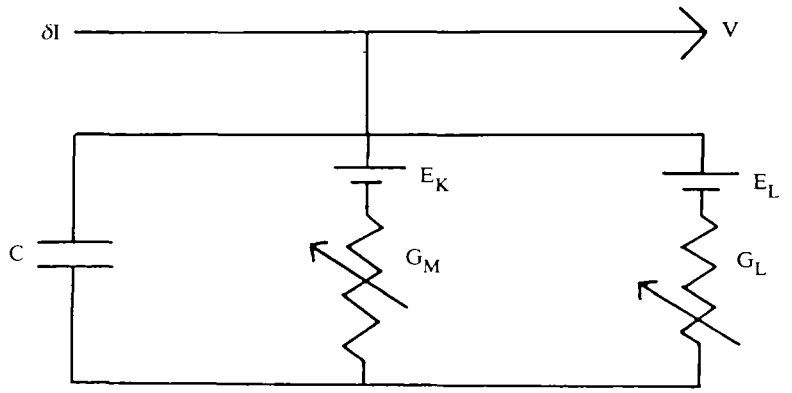

Fig. 8. Circuit diagram for linearized response of the ganglion cell membrane.

leakage conductance, presumably through shutting of voltage-independent Na^+ or Cl^- channels. Muscarine itself can produce similar decreased leakage outward currents in chloride-loaded rat sympathetic cells (Brown & Selyanko, 1985). In bullfrog C cells the decreased leakage may be followed by a period of increased leakage similar to that seen in B cells.

EXCITABILITY EFFECTS OF NEUROTRANSMITTERS IN B CELLS

We are now in a position to consider how inhibition of I_M, and to a lesser extent of I_{AHP}, might produce the dramatic changes in firing pattern that are seen during slow synaptic potentials or receptor stimulation. It is simplest to start by considering the subthreshold responses that occur during very weak direct current inputs or small fEPSPs. The normal resting potential of B cells is still somewhat uncertain, but is probably −55 to −60 mV, so that a small, standing M current is already present (but see Tosaka, Takasa, Miyazaki & Libet, 1983). An applied weak current step will cause the membrane potential to deviate from rest as a result of charging the membrane capacity. However, the fraction of M channels open is no longer appropriate to the new membrane potential, and this fraction will relax slowly, causing the potential to sag back towards its original value. To compute the exact time course of the potential trajectory one must solve the equations describing current flow in the circuit diagram shown in Fig. 8.

G_M is a time- and voltage-dependent conductance, whereas the other values are fixed. The following equation applies (δI is the applied current step):

$$\delta I = C\,dV/dt + G_L(V - E_L) + G_M(V - E_K). \quad (1)$$

G_M is considered to be equal to the product of the maximum available M conductance (typically 85 nS) and the fraction of M channels that are open at any moment, x_M. Because opening or closing of M channels in voltage-clamp experiments follows an exponential time course, a simple, first-order differential equation adequately describes the time course of x_M:

$$dx_M/dt = (x_{M,\infty} - x_M)/\tau_M, \quad (2)$$

where $x_{M,\infty}$ is the steady-state fractional activation of the M conductance, and τ_M is the time constant for activation/deactivation at any given voltage. Thus the key information which must be obtained in voltage-clamp experiments is the voltage dependence of $x_{M,\infty}$ and τ_M. Fortunately these details are available in the range -100 to -20 mV (Adams *et al.* 1982*a*), and have been recently extended to more positive potentials (Lancaster & Pennefather, 1986).

The strong voltage dependence of τ_M and $x_{M,\infty}$ precludes general analytical solution of equations 1 and 2. However, if the injected current step I is very small, the membrane potential always stays very close to its original value, so that τ_M is practically constant, and $x_{M,\infty}$ is a roughly linear function of voltage. The equations can thus be linearized and solved to yield:

$$\delta V = \delta I(Ae^{-t/\tau_1} + Be^{-t/\tau_2}), \tag{3}$$

where A, B, τ_1 and τ_2 are algebraic functions of all the circuit parameters and the slope of the $x_{M,\infty}$ curve at rest potential. For typical values of these parameters a double exponential (overdamped oscillation) or highly damped oscillation is expected, just as is observed in real cells. Intuitively one can see why this should be so. Over most of its activation range τ_M is considerably larger than the effective cell membrane time constant $C/(G_L + G_M x_{M,\infty})$ so that the potential step produces an initial fast displacement which relaxes back to a steady-state value as M channels open or close.

The general shape of the response is much the same even for larger current steps which do not allow linearization. These potential trajectories have been obtained by numerical integration of the above equations 1 and 2 (Adams *et al.* 1982*a*,*b*,*c*).

The linearization approach, or alternatively numerical integration, can also be used to calculate the voltage trajectories generated by brief current inputs, such as small fEPSPs. These calculations predict that subthreshold EPSPs should be followed by a small hyperpolarizing bounce, if the initial membrane potential is within the M activation range. This bounce is quite different from the afterhyperpolarization that follows massive iontophoretic ACh applications, which is due to calcium entry through the nicotinic channels and activation of $G_K(Ca)$ (Tokimasa & North, 1984). The absence of the fEPSP afterbounce in external records from whole ganglia may indicate that the normal resting potential of unimpaled cells is at least -60 mV (Tosaka *et al.* 1983).

These calculations do not predict the membrane potential responses to larger depolarizing or hyperpolarizing current steps, or to normal strength synaptic inputs, since they do not incorporate the other six voltage-dependent currents. To extend the simulations it is necessary to have equations similar to 1 and 2 above for each conductance. Unfortunately all the other conductances show more complex kinetics than G_M, and in no case does a complete description exist. However, in each case enough quantitative information is available to develop adequate approximate descriptions. The simplest are the purely voltage-dependent systems G_{Na}, G_K and G_A. These are modelled in a conventional Hodgkin–Huxley manner by including

inactivation variables. Our equations for G_K and G_A are firmly based on our own measurements, while provisionally we have adapted the Frankenheuser–Huxley equations for nodal G_{Na} to the overall time course of I_{Na} in bullfrog neurones. Activation and inactivation kinetics were slowed by a factor of two and shifted in the depolarizing direction. Ultimately it should be possible to incorporate the more detailed analysis of inactivation referred to above.

G_{Ca}, G_C and G_{AHP} are more difficult to model because each depends, *inter alia*, on the subsurface calcium concentration. In general we have made the simplest possible assumptions consistent with our data, i.e. activation (or in the case of G_{Ca}, inactivation) by calcium binding:

$$Ca + R \rightleftharpoons CaR^*.$$

In the case of G_{AHP}, it was necessary to assume that cooperative calcium binding was needed for the channel opening, to account for the almost complete activation produced by brief depolarizations. The kinetics of G_C and G_{AHP} activation are thus governed by the calcium binding/unbinding reactions, endowed in the former case with suitable voltage dependence. In the case of G_{Ca}, the calcium blocking reaction

$$Ca + (R^* + R) \rightleftharpoons CaR$$

was assumed to be instantaneous.

The diffusion of calcium within the cell was represented by a simplified two-compartment system (Fig. 9). Both intracellular compartments were assumed to contain a calcium buffer of plausible amount and binding rate constants, and calcium was extruded across the cell membrane in a voltage-dependent manner.

Intact ganglion cells are surrounded by a tight glial capsule which greatly restricts the escape of potassium ions from the cell surface. This was represented as another well-mixed compartment around the plasmalemma (see Fig. 9). The thickness and permeability of this compartment were estimated experimentally by varying

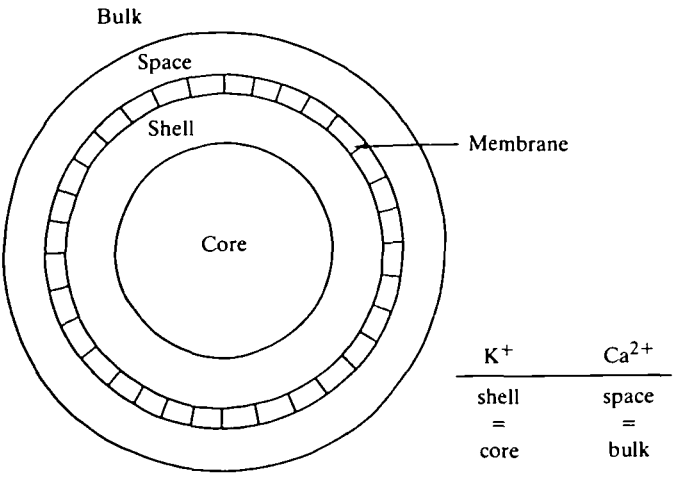

Fig. 9. Compartment model of ion diffusion in bullfrog ganglion cells.

the length of 'loading' depolarizations and measuring the resulting change in E_K (Lancaster & Pennefather, 1986).

Before considering the detailed behaviour of the computer model it would be well to consider in a qualitative manner how the various conductances might interact to generate complex trajectories such as action potentials, and how blocking specific channels might be expected to modify the observed responses. The response to prolonged hyperpolarizing inputs is fairly simple to understand. If the initial potential is positive to −60 mV, i.e. within the activation range of I_M and I_A, small steps will generate trajectories just like those described above for I_M alone, whereas large steps, which remove I_A inactivation, will be followed by a notch on the repolarizing phase (Connor & Stevens, 1971), just as is seen in real cells.

Brief suprathreshold depolarizing inputs generate spikes whose upswing (typically 100–500 $V s^{-1}$: Akasu *et al.* 1983*a*,*b*; MacDermott & Weight, 1982) is determined mainly by the cell capacity and the maximum sodium current (approx. 20 nA). The capacity of intact cells in whole isolated ganglia is typically 400 pF, larger than expected from the apparent cell diameter, and also larger than seen in acutely dissociated cells (approx. 100 pF: S. W. Jones & W. Gruner, unpublished observations). Presumably this reflects the contribution of initial segment membrane, although it is unclear quite how isopotential this compartment is with the soma (see Adams *et al.* 1982*a*,*b*,*c*). If it is not isopotential then the question of channel distribution would become important. In other cell types there is evidence for preferential localization of Na^+ channels in the initial segment (Matsumoto & Rosenbluth, 1985).

The action potential repolarizes at an almost comparable rate (50 $V s^{-1}$), whereas sodium inactivation alone could only allow repolarization at a rate equal to the reciprocal of the cell time constant. Clearly a large outward current must activate during the spike itself, and there are only two possible candidates, I_K and I_C. Of course in squid axon, I_K (together with sodium inactivation) repolarizes the spike, but this does not seem to be the case in bullfrog neurones, because activation of I_K takes several milliseconds. Brief spike-like depolarizations only activate I_C and, correspondingly, application of calcium blockers reduces the repolarization rate as well as the maximum hyperpolarizing excursion (which now occurs somewhat later; Fig. 3, cf. Fig. 10). The fact that even after block of calcium entry, spike repolarization still occurs rapidly, albeit at a reduced rate, presumably reflects enhanced recruitment of I_K by the broadened spike. TEA prolongs the spike to about the same extent as calcium deprivation. Since TEA is equally effective in blocking I_C and I_K, this must mean that spike broadening enhances Ca^{2+} entry enough to restore I_C to at least its control level. If TEA is applied to a Ca^{2+}-deprived cell, further spike broadening is seen, and Na^+ inactivation, I_M and even I_{AHP} become the main repolarizing influences.

After the normal spike has reached its maximum hyperpolarizing excursion, G_C must return rapidly to zero, even though the internal calcium concentration remains transiently elevated (e.g. Smith, MacDermott & Weight, 1983). At −80 mV the I_C tail current has a time constant of only 1 ms, and were it not for I_{AHP} the spike AHP

would decay passively back to rest. Indeed, in our early work this was usually the case, because unsuspected damage had eliminated or obscured the effect of I_{AHP}. Even here, however, the decay is not completely passive, because the AHP itself is long and large enough to turn off some of the standing M conductance, resulting in a brief depolarizing afterbounce.

Lightly damaged cells, possessing a normal I_{AHP}, show a slow component in the AHP decay. The exact shape of the AHP following its initial excursion is rather variable and this variability correlates with the degree of damage the cell has sustained. Rather leaky cells show an initially fast decaying AHP with a slow tail. The slow tail becomes proportionately larger as the leak decreases, until no fast decay is present. Even less leaky cells show an additional rising phase to the AHP (i.e. arising out of the initial hyperpolarizing excursion) followed by a slow decay phase. These various complex waveforms arise purely from variations in the passive leak resistance, and not the underlying ionic conductances, as shown by a passive model of the cell membrane (Adams, Pennefather & Lancaster, 1985; Adams & Galvan, 1986).

We are now in a position to consider the pattern of discharge expected during a *maintained* depolarizing stimulus. The first spike occurs as described above, and is followed by a brief hyperpolarization, which brings the potential below rest. If the cell has little or no I_{AHP}, this is followed by a short, overshooting depolarization, which could reflect partly the normal sag that occurs in a subthreshold depolarizing electrotonic potential, and partly turning off of M channels during the early spike afterhyperpolarization. The overshooting depolarizing 'bounce' then settles down to a maintained level of depolarization which is largely determined by the steady-state, current/voltage relationship. This level is normally subthreshold, because development of outward M current subtracts from the applied stimulus current.

If AHP current is present this will be triggered by the initial spike, and will mask the afterdepolarizing bounce and prevent further spiking. Both I_M and I_{AHP} act by subtracting from the stimulus. I_{AHP} acts early on because it is activated by calcium entry. Adaptation by this mechanism has the drawback that it wears off since the calcium load is rapidly dissipated. I_M takes time to develop but then continues to act. These two currents thus play complementary roles in adaptation. Alone neither could produce complete adaptation but together they effectively limit firing.

COMPUTER SIMULATIONS

The qualitative analyses and predictions in the preceding section have been tested and refined by the detailed computer simulations. The interpretation of the repolarization and AHP of the action potential given above is completely borne out by these calculations. Both I_C and I_K appear as brief outward currents coincident with repolarization, I_C being normally much the larger (20 nA *vs* 5 nA). However, inhibition of Ca^{2+} entry considerably reduces I_C, with a compensatory increase in I_K due to slight spike broadening (Fig. 10). I_C by no means disappears because at positive potentials resting internal calcium is adequate to allow some activation.

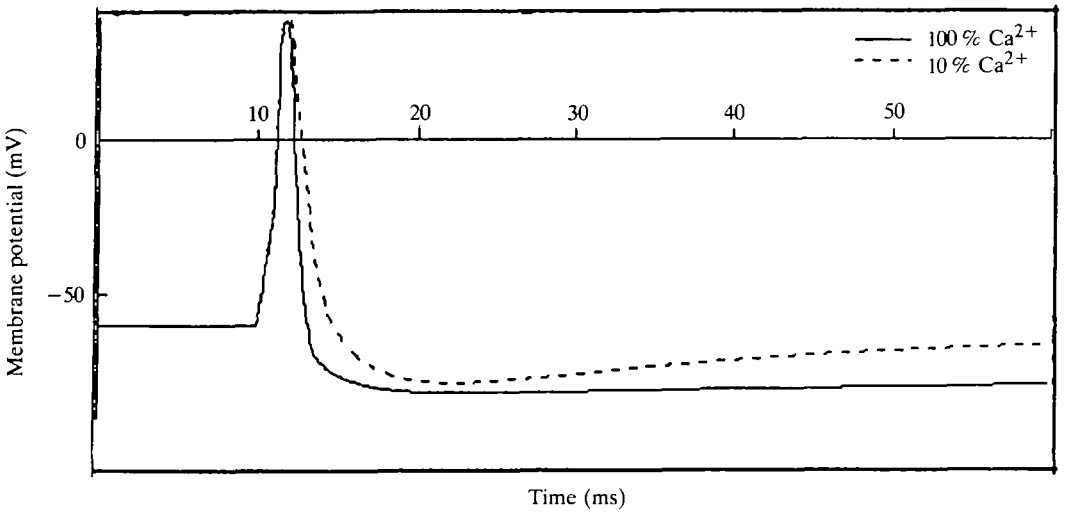

Fig. 10. Computer simulation of effect of calcium-deprivation on the time course of the action potential. The model cell was 'manually clamped' to −60 mV and a spike elicited by a brief current pulse. Compare with Fig. 3.

Similarly, in voltage-clamp experiments (Lancaster & Pennefather, 1986) or simulations, considerable I_C can be triggered by large depolarizations in the presence of cadmium.

The only other outward current significantly activated by single spikes according to this model is I_{AHP}. As observed experimentally this shows: (1) only a very brief rising phase, (2) near maximal activation by single spikes and (3) exponential decay which gets slower following a burst of spikes. As expected, the form of the AHP following single spikes depends critically on input resistance.

The calculations also confirm the synergistic actions of I_M and I_{AHP} in producing spike frequency adaptation during long current pulses. Inhibition of I_M allows the firing of isolated extra spikes late in the depolarizing pulse, while inhibition of I_{AHP} produces rather little increase in firing. But inhibition of I_{AHP} does allow the observation of a depolarizing 'bounce' following the initial spike. This bounce is most prominent when the empirically determined voltage dependence of M activation at positive potentials (Lancaster & Pennefather, 1986) is used, as opposed to the original extrapolation of data in the negative potential range (Adams *et al.* 1982*a*). This is because, in the original formulation, considerable M activation can occur during the spike itself. Ideally (and in fact experimentally) one would want little net change in the M-activation variable during *single* spikes, with activation (during the upswing) just balancing deactivation (during the afterhyperpolarization). This would allow a gradual and sustained increase in I_M during the depolarizing pulse.

As expected, inhibition of *both* I_{AHP} and I_M allows sustained repetitive firing during the pulses (Fig. 11). In real cells, firing does cease after 1 or 2 s, presumably because of slow sodium inactivation processes not yet incorporated in the computer program. These predicted effects of separate or combined inhibition of I_M and I_{AHP}

have been experimentally verified using curare and/or muscarine as relatively selective blockers (Pennefather, Jones & Adams, 1985*a*). It should be noted that in our early work (Brown & Adams, 1980; Adams *et al.* 1982*b*) inhibition of I_M alone was enough to allow repetitive firing, because these cells were somewhat damaged and lacked I_{AHP}.

CONCLUSIONS

Our knowledge of synaptic transmission and excitability characteristics in frog sympathetic ganglia is probably now more complete than in any other comparable miniature nervous system. The way that the fast and slow synaptic potentials generate electrical activity, and the interactions between them, is now reasonably well understood. Nevertheless, our ignorance remains daunting. Many of the suspected channels have not yet been identified in individual recordings. The biochemical coupling mechanisms are only beginning to be explored. Perhaps most acutely, the physiological relevance of these elaborate phenomena to normal impulse traffic across the ganglion and to target tissues such as blood vessels and slime glands is quite obscure. Even if, in these ganglia, the phenomena discussed in this chapter have little functional importance, it is now clear that very similar processes occur in mammalian central neurones such as rodent hippocampal pyramidal cells (Halliwell & Adams, 1982; Cole & Nicoll, 1984; Madison & Nicoll, 1984; Lancaster & Adams, 1986; Gähwiler & Brown, 1985) and human neocortical neurones (Halliwell, 1986).

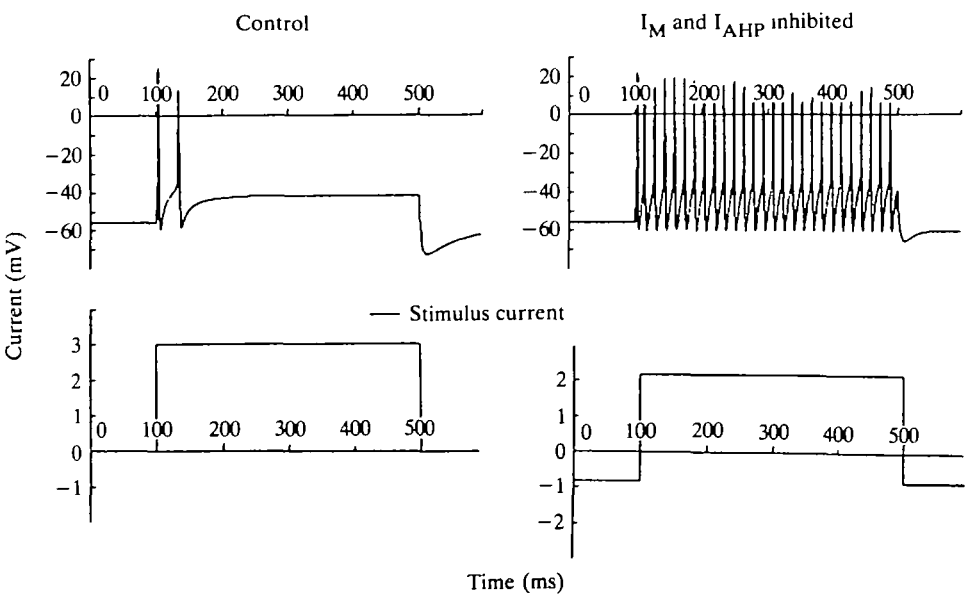

Fig. 11. Computer simulation of repetitive firing in a B cell. Manual clamp to −60 mV resting potential. The control model fires only two spikes to a 3 nA current pulse, but maintained firing is seen after inhibition of I_M and I_{AHP}. Compare with Fig. 2.

Slow synaptic modulation of voltage-dependent conductances is likely to become an increasingly attractive theme for investigation.

This work was supported by NIH grants NS 18579 (PRA) and NS 20751 (SWJ). The manuscript was prepared during a visit to the Instituto de Investigaciones Bioquimicas, Bahia Blanca, supported by the CONICET of Argentina. PRA thanks F. J. Barrantes for his hospitality and M. H. Salaberry de Saint-Lary and L. Nielsen for their help with the manuscript. Further help was provided by Dahl Capello.

REFERENCES

ADAMS, P. R. & BROWN, D. A. (1980). Luteinizing hormone-releasing factor and muscarinic agonists act on the same voltage-sensitive K^+-current in bullfrog sympathetic neurones. *Br. J. Pharmac.* **68**, 353–355.

ADAMS, P. R. & BROWN, D. A. (1982). Synaptic inhibition of the M-current: Slow excitatory postsynaptic potential mechanism in bullfrog sympathetic neurones. *J. Physiol., Lond.* **332**, 263–272.

ADAMS, P. R. & BROWN, D. A. (1986). Effects of phorbol ester on slow potassium currents of bullfrog ganglion cells. *Biophys. J.* **49**, 215a.

ADAMS, P. R., BROWN, D. A. & CONSTANTI, A. (1982*a*). M-currents and other potassium currents in bullfrog sympathetic neurones. *J. Physiol., Lond.* **330**, 537–572.

ADAMS, P. R., BROWN, D. A. & CONSTANTI, A. (1982*b*). Pharmacological inhibition of the M-current. *J. Physiol., Lond.* **332**, 223–262.

ADAMS, P. R., BROWN, D. A., CONSTANTI, A., CLARK, R. B. & SATIN, L. (1984). Calcium-activated potassium channels in bullfrog sympathetic ganglion cells. In *Calcium in Biological Systems* (ed. R. Rubin). New York: Plenum Press.

ADAMS, P. R., BROWN, D. A. & JONES, S. W. (1983). Substance P inhibits the M-current in bullfrog sympathetic neurones. *Br. J. Pharmac.* **79**, 330–333.

ADAMS, P. R., CONSTANTI, A., BROWN, D. A. & CLARK, R. B. (1982*c*). Intracellular Ca^{2+} activates a fast voltage-sensitive K^+ current in vertebrate sympathetic neurones. *Nature, Lond.* **296**, 746–749.

ADAMS, P. R. & GALVAN, M. (1986). Voltage-dependent currents of vertebrate neurones and their role in membrane excitability. *Advances in Neurology*, vol. 44 (ed. A. V. Delgado-Escueta, A. A. Ward Jr, D. M. Woodbury & R. J. Porter). New York: Raven Press.

ADAMS, P. R., PENNEFATHER, P. & LANCASTER, B. (1985). Spike after hyperpolarization (AHPs) in bullfrog sympathetic ganglion "B" cells. *Biophys. J.* **47**, 387a.

AKASU, T., GALLAGHER, J. P., KOKETSU, K. & SHINNICK-GALLAGHER, P. (1984). Slow excitatory post-synaptic currents in bullfrog sympathetic neurones. *J. Physiol., Lond.* **351**, 583–593.

AKASU, T., HIRAI, K. & KOKETSU, K. (1983*a*). Modulatory actions of ATP on membrane potentials of bullfrog sympathetic ganglion cells. *Brain Res.* **258**, 313–317.

AKASU, T., NISHIMURA, T. & KOKETSU, K. (1983*b*). Substance P inhibits the action potentials in bullfrog sympathetic ganglion cells. *Neurosci. Letts* **41**, 161–166.

BARRETT, J. M., MAGLEBY, K. L. & PALLOTTA, B. S. (1982). Properties of calcium-activated potassium channels in cultured rat muscle. *J. Physiol., Lond.* **331**, 211–230.

BARRY, S. R., WERZ, M. A. & MACDONALD, R. L. (1983). Slow voltage dependent potassium conductance in sensory neurons is muscarine insensitive. *Soc. Neurosci. Abstr.* **9**, 500.

BOSSU, J. L. & FELTZ, H. (1984). Patch-clamp study of the tetrodotoxin-resistant sodium current in group C sensory neurones. *Neurosci. Letts* **51**, 241–246.

BREITWIESER, G. E. & SZABO, G. (1985). Uncoupling of cardiac muscarinic and β-adrenergic receptors from ion channels by aguarine nucleotide analogue. *Nature, Lond.* **317**, 538–540.

BROWN, D. A. & ADAMS, P. R. (1980). Muscarinic suppression of a novel voltage-sensitive K^+-current in a vertebrate neurone. *Nature, Lond.* **283**, 673–676.

BROWN, D. A., CONSTANTI, A. & ADAMS, P. R. (1982). Calcium-dependence of a component of transient outward current in bullfrog ganglion cells. *Soc. Neurosci. Abstr.* **8**, 252.

BROWN, D. A. & SELYANKO, A. A. (1985). Two components of muscarine-sensitive membrane current in rat sympathetic neurones. *J. Physiol., Lond.* (in press).

COOK, N. S. & HAYLETT, D. G. (1985). Effects of apamin, quinine and neuromuscular blockers on calcium-activated potassium channels in guinea-pig hepatocytes. *J. Physiol., Lond.* **358**, 373–394.

COLE, A. E. & NICOLL, R. (1984). Characterization of a slow cholinergic post-synaptic potential recorded *in vitro* from rat hippocampal pyramidal cells. *J. Physiol., Lond.* **352**, 173–188.

CONNOR, J. A. & STEVENS, C. F. (1971). Prediction of repetitive firing behaviour from voltage clamp data on an isolated neurone soma. *J. Physiol., Lond.* **213**, 31–53.

DODD, J. & HORN, J. P. (1983*a*). A reclassification of B and C neurones in the 9th and 10th paravertebral sympathetic ganglia of the bullfrog. *J. Physiol., Lond.* **334**, 225–269.

DODD, J. & HORN, J. P. (1983*b*). Muscarinic inhibition of sympathetic C neurones in the bullfrog. *J. Physiol., Lond.* **334**, 271–291.

DUBOIS, J. M. (1981). Evidence for the existence of three types of potassium channels in the frog Ranvier node membrane. *J. Physiol., Lond.* **318**, 297–316.

EIDEN, L. E. & ESKAY, R. L. (1980). Characterization of LRF-like immunoreactivity in the frog sympathetic ganglia: non-identity with LRF decapeptide. *Neuropeptides* **1**, 29–37.

GAHWILER, B. H. & BROWN, D. A. (1985). Functional innervation of cultured hippocampal neurones by cholinergic afferents from co-cultured septal explants. *Nature, Lond.* **313**, 577–579.

HALLIWELL, J. V. (1986). Current and voltage responses from human neocortical neurones *in vitro*. *J. Physiol., Lond.* (in press).

HALLIWELL, J. V. & ADAMS, P. R. (1982). Voltage-clamp analysis of muscarinic excitation in hippocampal neurons. *Brain Res.* **250**, 71–92.

HARTZELL, H. C. (1980). Distribution of muscarinic acetylcholine receptors and presynaptic nerve terminals in amphibian heart. *J. Cell Biol.* **86**, 6–20.

HORWITZ, J., TSYMBABOV, S. & PERLMAN, R. L. (1984). Muscarine increases tyrosine 3-monoxygenase activity and phospholipid metabolism in the superior cervical ganglion of the rat. *J. Pharmac. exp. Ther.* **229**, 577–582.

HUGUES, M., SCHMID, H., ROMEY, G., DUVAL, D., FRELIN, C. & LAZDUNSKI, M. (1982). The Ca^{2+}-dependent slow K^+ conductance in cultured rat muscle cells: characterization with apamin. *EMBO J.* **1**, 1039–1042.

JAN, L. Y. & JAN, Y. N. (1982). Peptidergic transmission in sympathetic ganglia of the frog. *J. Physiol., Lond.* **327**, 219–246.

JAN, Y. N., JAN, L. Y. & KUFFLER, S. W. (1979). A peptide as possible transmitter in sympathetic ganglia of the frog. *Proc. natn. Acad. Sci. U.S.A.* **76**, 1501–1505.

JAN, Y. N., JAN, L. Y. & KUFFLER, S. W. (1980). Further evidence for peptidergic transmission in sympathetic ganglia. *Proc. natn. Acad. Sci. U.S.A.* **77**, 5008–5012.

JENKINSON, D. H., HAYLETT, D. G. & COOK, N. S. (1983). Calcium-activated potassium channels in liver cells. *Cell Calcium* **4**, 429–437.

JONES, S. W. (1984). Muscarinic and peptidergic actions on C cells of bullfrog sympathetic ganglia. *Soc. Neurosci. Abstr.* **10**, 207.

JONES, S. W. (1985). Muscarinic and peptidergic excitation of bullfrog sympathetic neurones. *J. Physiol., Lond.* **366**, 63–87.

JONES, S. W., ADAMS, P. R., BROWNSTEIN, M. J. & RIVIER, J. E. (1984). Teleost luteinizing hormone-releasing hormone: action on bullfrog sympathetic ganglia is consistent with role as neurotransmitter. *J. Neurosci.* **4**, 420–429.

KATAYAMA, Y. & NISHI, S. (1982). Voltage-clamp analysis of peptidergic slow depolarizations in bullfrog sympathetic ganglion cells. *J. Physiol., Lond.* **333**, 305–313.

KOKETSU, K. (1984). Modulation of receptor sensitivity and action potentials by transmitters in vertebrate neurones. *Jap. J. Physiol.* **34**, 945–960.

KUBA, K. (1980). Release of calcium ions linked to the activation of potassium conductance in a caffeine-treated sympathetic neurone. *J. Physiol., Lond.* **298**, 251–269.

KUBA, K. & KOKETSU, K. (1978). Synaptic events in sympathetic ganglia. *Prog. Neurobiol.* **11**, 77–169.

KUBA, K. & NISHI, S. (1979). Characteristics of fast excitatory postsynaptic currents in bullfrog sympathetic ganglion cells. *Pflügers Arch. ges. Physiol.* **378**, 205–212.

KUFFLER, S. W. & SEJNOWSKI, T. J. (1983). Peptidergic and muscarinic excitation at amphibian sympathetic synapses. *J. Physiol., Lond.* **341**, 257–278.

LANCASTER, B. & ADAMS, P. R. (1986). Calcium-dependent current generating the afterhyperpolarization of hippocampal neurons. *J. Neurophysiol.* (in press).

LANCASTER, B. & PENNEFATHER, P. (1986). Potassium currents in bullfrog ganglion cells evoked by brief depolarizations. *J. Physiol., Lond.* (in press).

LAND, B. R., SALPETER, E. E. & SALPETER, M. M. (1981). Kinetic parameters for acetylcholine interaction in intact neuromuscular junction. *Proc. natn. Acad. Sci. U.S.A.* **78**, 7200–7204.

MACDERMOTT, A. B., CONNOR, E. A., DIONNE, V. E. & PARSONS, R. L. (1980). Voltage clamp study of fast excitatory synaptic currents in bullfrog sympathetic ganglion cells. *J. gen. Physiol.* **75**, 39–60.

MACDERMOTT, A. B. & WEIGHT, F. F. (1982). Action potential repolarization may involve a transient, Ca^{2+}-sensitive outward current in a vertebrate neurone. *Nature, Lond.* **296**, 746–749.

MADISON, D. V. & NICOLL, R. A. (1984). Control of the repetitive discharge of rat CA1 pyramidal neurones *in vitro*. *J. Physiol., Lond.* **354**, 319–331.

MARSHALL, L. M. (1981). Synaptic localization of a bungarotoxin binding which blocks nicotinic transmission at frog sympathetic neurones. *Proc. natn. Acad. Sci. U.S.A.* **78**, 1948–1952.

MARSHALL, L. M. (1985). Presynaptic control of synaptic channel kinetics in sympathetic neurones. *Nature, Lond.* **317**, 612–623.

MARTY, A. (1981). Ca-dependent K channels with large unitary conductance in chromaffin cell membranes. *Nature, Lond.* **291**, 497–500.

MATSUMOTO, E. & ROSENBLUTH, J. (1985). Plasma membrane structure at the axon hillock, initial segment and cell body of frog dorsal root ganglion cells. *J. Neurocytol.* **14**, 731–747.

MILLER, C., MOCZYDLOWSKI, E., LATORRE, R. & PHILLIPS, M. (1985). Charybdotoxin, a protein inhibitor of single Ca^{2+}-activated I_K channels from mammalian skeletal muscle. *Nature, Lond.* **313**, 316–319.

MOCZYDLOWSKI, E. & LATORRE, R. (1983). Gating kinetic of Ca^{2+} activated K^+ channels from rat muscle incorporated into planar lipid bilayer membranes: Evidence for two voltage dependent Ca^{2+} binding reactions. *J. gen. Physiol.* **82**, 511–542.

NEHER, E. (1971). Two fast transient current components during voltage clamp on snail neurones. *J. gen. Physiol.* **58**, 36–53.

NOHMI, M. & KUBA, K. (1984). (+)-Tubocurarine blocks the Ca^{2+}-dependent K^+-channel of the bullfrog sympathetic ganglion cell. *Brain Res.* **301**, 146–148.

NOWYCKY, M. C., FOX, A. P. & TSIEN, R. W. (1983). Three types of neuronal calcium channel with different calcium agonist sensitivity. *Nature, Lond.* **316**, 440–443.

PALLOTTA, B. S. (1985). Calcium-activated potassium channels in rat muscle inactivate from a short duration open state. *J. Physiol., Lond.* **363**, 501–516.

PENNEFATHER, P., JONES, S. W. & ADAMS, P. R. (1985*a*). Modulation of repetitive firing in bullfrog sympathetic ganglion cells by two distinct K currents, I_M and I_{AHP}. *Soc. Neurosci. Abstr.* **11**, 148.

PENNEFATHER, P., LANCASTER, B., ADAMS, P. R. & NICOLL, R. A. (1985*b*). Two distinct Ca-dependent K currents in bullfrog sympathetic ganglion cells. *Proc. natn. Acad. Sci. U.S.A.* **82**, 3040–3044.

PFAFFINGER, P. J., MARTIN, J. M., HUNTER, D. D., NATHANSON, N. M. & HILLE, B. (1985). GTP-binding proteins couple cardiac muscarinic receptors to a K channel. *Nature, Lond.* **317**, 536–539.

ROMEY, G. & LAZDUNSKI, M. (1984). The coexistence in rat muscle cells of two distinct classes of Ca^{2+}-dependent K^+ channels with different pharmacological properties and different physiological functions. *Biochem. biophys. Res. Commun.* **118**, 669–674.

SAKMANN, B., NOMA, A. & TRAUTWEIN, W. (1983). Acetylcholine activation of single muscarinic K^+ channels in isolated pacemaker cells of the mammalian heart. *Nature, Lond.* **303**, 250–253.

SALKOFF, L. (1983). Ion currents in *Drosophila* flight muscle. *J. Physiol., Lond.* **337**, 687–696.

SARGENT, P. B. (1983). The number of synaptic boutons terminating on *Xenopus* cardiac ganglion cells is directly correlated with cell size. *J. Physiol., Lond.* **343**, 85–104.

SHERWOOD, N., EIDEN, L., BROWNSTEIN, M., SPIESS, J., RIVIER, J. & VALE, W. (1983). Characterization of a teleost gonadotropin-releasing hormone. *Proc. natn. Acad. Sci. U.S.A.* **80**, 2794–2798.

SCHULMAN, J. & WEIGHT, F. (1976). Synaptic transmission: Long-term potentiation by a postsynaptic mechanism. *Science* **194**, 1437–1439.

SMITH, S. J., MACDERMOTT, A. B. & WEIGHT, F. F. (1983). Detection of intracellular Ca^{2+} transients in sympathetic neurones using arsenazo III. *Nature, Lond.* **304**, 350–352.

STREB, H., IRVINE, R. F., BERRIDGE, M. J. & SCHULZ, I. (1983). Release of Ca^{2+} from a nonmitochondrial intracellular store in pancreatic acinar cells by inositol 1,4,5-trisphosphate. *Nature, Lond.* **306**, 67–69.

TOKIMASA, T. (1984). Muscarinic agonists depress calcium dependent g_K in bullfrog sympathetic neurons. *J. auton. nerv. Syst.* **10**, 107–116.

TOKIMASA, T. (1985). Spontaneous muscarinic suppression of the Ca-activated K-current in bullfrog sympathetic neurons. *Brain Res.* **344**, 134–141.

TOKIMASA, T. & NORTH, R. A. (1984). Calcium entry through acetylcholine-channels can activate potassium conductance in bullfrog sympathetic neurons. *Brain Res.* **295**, 364–367.

TOSAKA, T., TAKASA, J., MIYAZAKI, T. & LIBET, B. (1983). Hyperpolarization following activation of K^+ channels by excitatory postsynaptic potentials. *Nature, Lond.* **308**, 143–150.

VICENTINI, L. M., DI VIRGILIO, F., AMBIOSINI, A., POZZAR, T. & MELDOLESI, J. (1985). Tumor promoter phorbol 12-myristate, 13-acetate inhibits phosphoinositide hydrolysis and cytosolic Ca^{2+} rise induced by the activation of muscarinic receptors in PC12 cells. *Biochem. biophys. Res. Commun.* **127**, 310–317.

WEIGHT, F. F. & VOTAVA, J. (1970). Slow synaptic excitation in sympathetic ganglion cells: evidence for synaptic inactivation of potassium conductance. *Science* **170**, 755–758.

WEITSEN, H. A. & WEIGHT, F. F. (1977). Synaptic innervation of sympathetic ganglion cells in the bullfrog. *Brain Res.* **128**, 197–211.